ISBN: 978-3-95450-231-8 ISSN: 2673-5490 doi: 10.18429/JACoW-IPAC2023-WEPA045

ARBITRARY TRANSVERSE AND LONGITUDINAL CORRELATION GENERATION USING TRANSVERSE WIGGLER AND WAKEFIELD STRUCTURES

G. Ha*, Northern Illinois University, Dekalb, IL, USA

Abstract

Transverse wigglers and wakefield structures are promising candidates for imparting arbitrary correlation on transverse and longitudinal phase spaces. They provide sinusoidal electromagnetic fields that become building blocks for Fourier synthesis. We present the progress of arbitrary correlation generation using transverse wiggler and wakefield structures.

INTRODUCTION

A particle beam's correlation can be considered part of a periodic function or a small fraction of a function with a large domain because the beam only exists locally. This implies that most of the beam's correlations can be approximated by the Fourier series or the summation of arbitrary cosines (i.e., cosine fitting). The development of methods or tools imparting sinusoidal modulation in the phase space would enable the generation of arbitrary two-dimensional correlations. Ref. [1] introduced a transverse wiggler as the tool to enable such manipulations.

The transverse wiggler is a 90°-rotated wiggler providing a vertical magnetic field along the x-direction [1, 2]. This magnet array can provide arbitrary modulation amplitude, period, and phase. Especially the modulation amplitude can be easily adjusted by controlling the gap, and the phase can be controlled by the wiggler's relative position to the beam axis. This flexibility of the transverse wiggler possibly realizes the generation of complex correlations such as the pattern in Fig. 1a.

Figure 1 is an example of generating desired correlation in the horizontal phase space using Fourier synthesis. A complex desired correlation is shown in panel a. We converted this pattern into a correlation with specific size and divergence (see panel b). The method is currently available for $x' = f(x)$ type correlations. Thus, the desired correlation in panel b was reverse-drifted, which is the target correlation for the Fourier synthesis (see panel c). This correlation is successfully approximated by Fourier series with 70 harmonics (see panel d). Then, it generates the desired correlation after the drift (see panel e). This method is applicable to any correlations following $x' = f(x)$.

In this paper, we present three exampled applications of arbitrary correlation generation; arbitrary spatial profile, linearization, and multiple beamlet generation. Contrary to Ref. [1], two additional examples are introduced in this paper. Also, the spatial profile shaping in this paper demonstrates the conversion of Gaussian profile to other profiles including

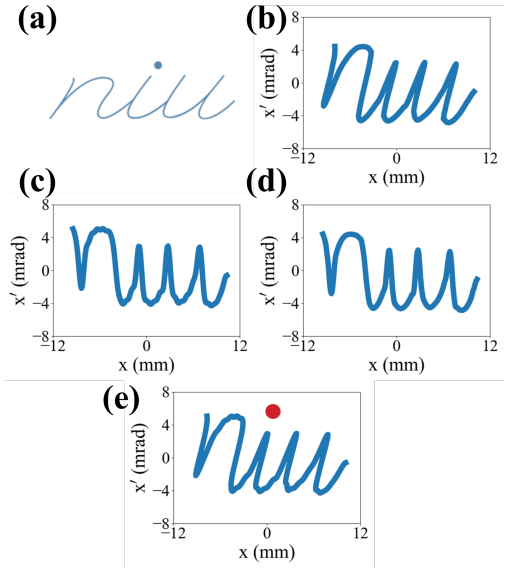

Figure 1: Approximation and generation of complex arbitrary correlation. (a) Target pattern to be printed in the horizontal phase space. (b) Desired correlation in the phase space. (c) Desired correlation after reversed drift for generating $x' = f(x)$ form. (d) Fourier approximation of the desired correlation in panel (c) using 70 harmonics. (d) Final correlation after the drift.

a doorstep profile for the first time. Note that the previously mentioned 70-harmonics is not practical. However, the examples given in the following sections implement ten or fewer modulators. If the transverse wiggler is the modulator, the longitudinal length of the modulator set usually does not exceed 10 cm. We also note that imparting sinusoidal modulation can also be achieved by accelerating fields that RF cavities [3] or wakefield structures generate [4]. However, they share the same principle as transverse wigglers but work in a different plane, so we do not distinguish them here. The particle tracking demonstration given in this paper only considered the linear transport of particles without any collective effects. Modulator thickness was ignored for simplicity.

EXAMPLE: ARBITRARY SPATIAL PROFILE

As described in Ref. [1], the target correlation can be obtained by solving the equation below.

$$N_f(R_{11}x_i + R_{12}F)\{R_{11} + R_{12}F'\} = N_i(x_i), \qquad (1)$$

* gwanghui.ha@gmail.com

ISBN: 978-3-95450-231-8 ISSN: 2673-5490 doi: 10.18429/JACoW-IPAC2023-WEPA045

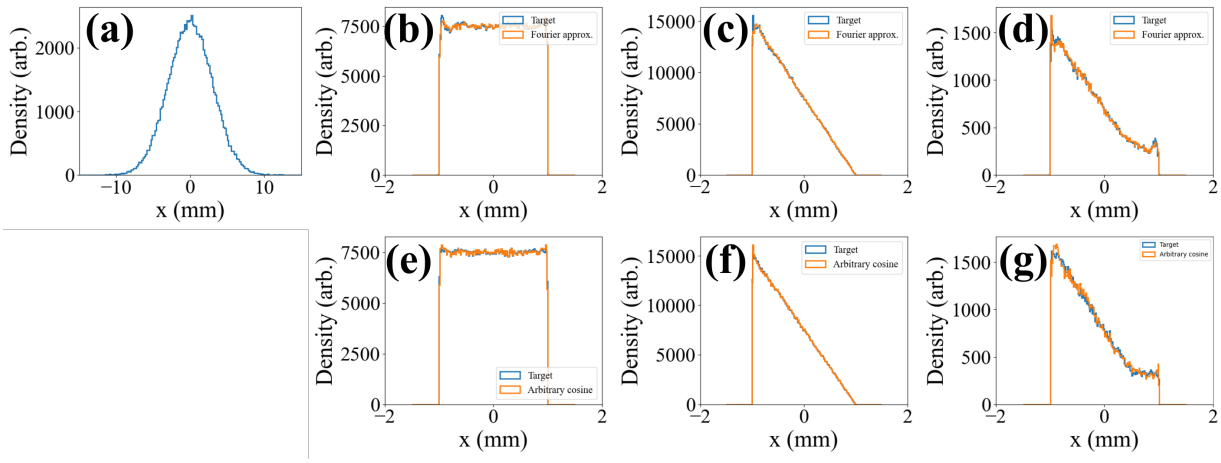

Figure 2: Conversion of Gaussian profile to uniform, triangle, and doorstep profiles. (a) Beam's initial horizontal profile. (b-d) Blue curves correspond to target profiles, and the beam's final horizontal profile are in orange. Here the required correlation was approximated by Fourier series with 24 harmonics. (e-g) Blue curves correspond to target profiles, and beam's final horizontal profile are in orange. The required correlation was approximated by the summation of arbitrary cosines. Total of five modulators were used for (e) and (f), and 7 modulators were used for (g).

where sub-index i and f denote the beam's initial and final position, and $N(x)$ is beam's one-dimensional profile, R_{mn} are transfer matrix from initial to final position, and $F(x)$ is the correlation function.

In this section, we show the conversion of a large Gaussian profile to small profiles with uniform, triangle, and doorstep shapes. The required correlation function (F) was calculated using Eq. 1. The correlation function was approximated by both Fourier series with 24 harmonics and several arbitrary cosines. In the case of arbitrary cosine, the differential evolution algorithm found the optimal cosine parameters. R_{11} and R_{12} were assumed to be 1 (i.e., transverse wiggler arrays both focused and shaped the beam).

The particle tracking results are shown in Fig. 2. The beam size was successfully focused from ±10 mm to ±1-1.5 mm. Fourier synthesis provided great matches of final profiles with target profiles (see panels b-d). More importantly, in the case of the uniform profile, horns coming from the tails of the Gaussian profiles are significantly suppressed (see Ref. [1]). The final profile has incredibly high uniformity. Also, this is the first time demonstrating doorstep profile generation from correlation-control approaches, which do not use masks. The results here prove the feasibility of very high-precision correlation-control-based shaping.

Contrary to the complex pattern in Fig. 1, desired correlation for the shaping is rather simple. In this case, the summation of arbitrary cosine can provide better performance with fewer modulators. Panels e-g show the particle tracking results from the arbitrary cosine sum concept. Here we approximated the desired correlation using several arbitrary cosines instead of Fourier series. Both uniform and triangle profiles required 5 modulators, and the doorstep profile required 7 modulators. This is a significant reduction of required modulators compared to the Fourier series case, which needed 24 modulators.

EXAMPLE: LINEARIZATION

Linearization is another representative application of correlation control, which has existed for a long time. However, conventional linearization (e.g., X-band linearizer [5]) only handles sinusoidal curvature from RF accelerating cavities. It is impossible to handle more complicated correlations (e.g., blue in Fig. 3a). On the other hand, the combination of transverse wiggler or wake structures can handle more complex correlations.

The example in this section deals with the correlation after the doorstep generation from the previous section. The blue dots in Fig. 3 show the phase space of the beam having a doorstep profile, which evolved from the Gaussian profile. Orange dots show the phase space after the linearization. The nonlinear curvature that the beam had after the shaping process is successfully linearized by eight modulators except for the periphery which initially had an extremely fast change of divergence. It would be possible to handle such patterns if we include high-frequency and high-amplitude cosines, but it is not practical. Instead, the periphery only contains <10% of the total charge and does not affect the profile. Thus, cutting the periphery would be a better choice (see Fig. 3b).

Note that the fast change pattern arises during the shaping process due to the initial Gaussian profile. Gaussian profiles have a long tail and it has to be folded to form a hard-edge in the periphery. Such a pattern would not appear in other more realistic initial profiles.

EXAMPLE: MULTI-BEAM AND SAWTOOTH CORRELATION

As sinusoidal modulations have been used for the bunch train generation, arbitrary correlation methods generate mul-

ISBN: 978-3-95450-231-8 ISSN: 2673-5490 doi: 10.18429/JACoW-IPAC2023-WEPA045

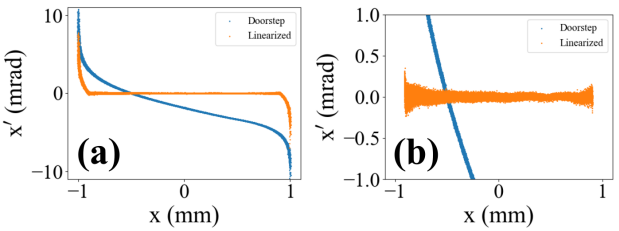

Figure 3: Linearization of final correlation from doorstep case. (a) the correlation from the doorstep case (blue) and the correlation after linearization (orange). (b) zoom-in picture of (a) with 10% cut of the periphery.

tiple beamlets in transverse and longitudinal planes. We introduce two examples in this section.

The first example shown in Fig. 4 is generating two bunches having different charges. We modified Halbach array's period to generate an unbalanced period and amplitude. This magnetic field successfully imparted two negative slopes that bunch the beam in a different level (see panel b). The phase space after the bunching (i.e., drift) is given in panel c, and the corresponding density profile is shown in panel d. The number of particles in the red box is about a factor of three lower than the number of particles in the blue box.

The simultaneous generation of bunches having different charge levels may be an interesting method for wakefield accelerators having tight drive-to-main timing tolerance [6]. As shown in the figure, it is possible to control the bunching level of each beamlet separately. Even though we do not demonstrate it here, combining the profile shaping and multiple beamlet generation can happen at the same time, which is a necessary process for collinear wakefield acceleration for efficiency improvement [7–12].

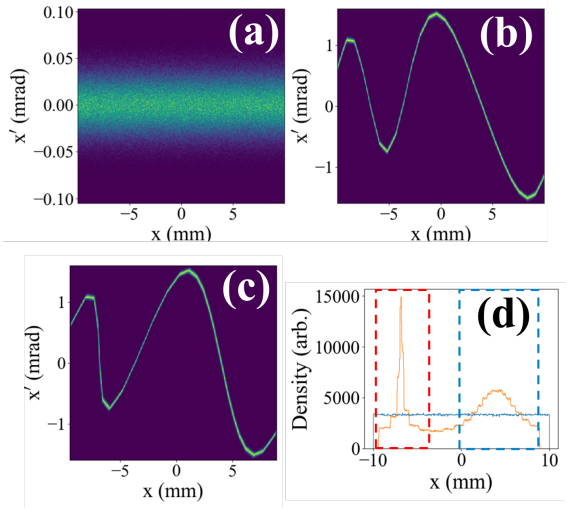

Figure 4: Generation of two beams having different charges. Panel a-c show Beam's horizontal phase spaces at different locations; (a) initial, (b) after modulator set, and (c) after drift. (d) Beam's horizontal profile corresponding to the panel c.

The second example is enhancing the bunching factor of bunch trains. In the case of widely adopted sinusoidal correlations, only a linear part of the sine-correlation, around $\lambda/4$ or less, contributes to forming density spikes. Particles outside the linear region generate a DC-like uniform base in the density profile. Minimizing this base level and making more particles contribute to density spikes requires minimizing the debunching region of the correlation and improving the linearity of the bunching region. A sawtooth correlation is an ideal correlation maximizing the bunching. The particle tracking result is shown in Fig. 5. A sawtooth correlation was generated by the combination of ten modulators. The result shows a significant drop in the base level and enhancement of density spikes.

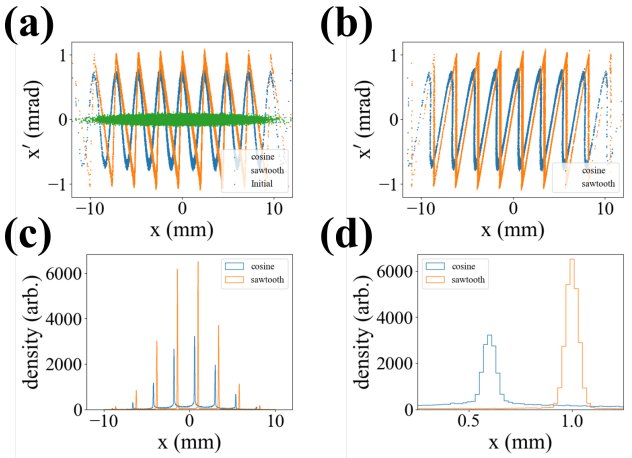

Figure 5: Cosine and sawtooth correlations and corresponding density profile after bunching. (a) shows beam's initial horizontal phase space (green) and ones after applying two different correlations; cosine (blue) and sawtooth (orange). (b) shows the phase spaces after a drift for maximum bunching. (c) shows corresponding density profiles and (d) is the zoom-in image of (c).

CONCLUSION

Arbitrary correlation generation is a highly feasible new method. Transverse wigglers and wakefield structures can impart sinusoidal modulation in transverse and longitudinal phase space, respectively. These designed correlations can be delivered to the other plane via emittance exchange too [13–15]. We introduced several applications of arbitrary correlation generation and their feasibility.

As mentioned earlier, the method is developed for $y = f(x)$ type correlations only. Thus, extending the method to generate arbitrary correlations having $F(x, y) = 0$ is the next step. It will require the use of quadrupole, drift, and other nonlinear magnets to shrink, stretch, rotate, and bend the phase space. Also, combining the method with transverse deflecting cavities or dipole magnets would provide a further extension of the method to 4-dimensional control.

ISBN: 978-3-95450-231-8 ISSN: 2673-5490 doi: 10.18429/JACoW-IPAC2023-WEPA045

REFERENCES

[1] G. Ha, M. Conde, and J. Power, "Arbitrary Transverse Profile Shaping using Transverse Wigglers," in *Proc. NA-PAC'2019)*, Lansing, MI, USA, Sep. 2019, pp. 403–406, doi:10.18429/JACoW-NAPAC2019-TUPLM15

[2] G. Ha, M. Conde, J. Power, J. Shao, and E. Wisniewski, "Tunable Bunch Train Generation Using Emittance Exchange Beamline With Transverse Wiggler," in *Proc. IPAC'2019*, Melbourne, VIC, Australia, May 2019, pp. 1612–1614, doi:10.18429/JACoW-IPAC2019-TUPGW089

[3] P. Piot *et al.*, "Generation and characterization of electron bunches with ramped current profiles in a dual-frequency superconducting linear accelerator," *Phys. Rev. Lett.*, vol. 108, p. 034 801, 2012, doi:10.1103/PhysRevLett.108.034801

[4] F. Mayet, R. Assmann, and F. Lemery, "Longitudinal phase space synthesis with tailored 3d-printable dielectric-lined waveguides," *Phys. Rev. Accel. Beams*, vol. 23, p. 121 302, 2020, doi:10.1103/PhysRevAccelBeams.23.121302

[5] P. Emma, "X-Band RF harmonic compensation for linear bunch compression in the LCLS," SLAC, San Francisco, CA, USA, Tech. Rep. SLAC-TN-05-004, LCLS-TN-01-1, Nov. 2001.

[6] G. Ha, J. G. Power, M. Conde, D. S. Doran, and W. Gai, "Simultaneous generation of drive and witness beam for collinear wakefield acceleration," *J. Phys. Conf. Ser.*, vol. 874, p. 012 027, 2017, doi:10.1088/1742-6596/874/1/012027

[7] Q. Gao *et al.*, "Observation of high transformer ratio of shaped bunch generated by an emittance-exchange beam line," *Phys. Rev. Lett.*, vol. 120, p. 114 801, 2018, doi:10.1103/PhysRevLett.120.114801

[8] G. Loisch *et al.*, "Observation of high transformer ratio plasma wakefield acceleration," *Phys. Rev. Lett.*, vol. 121, p. 064 801, 2018, doi:10.1103/PhysRevLett.121.064801

[9] R. Roussel *et al.*, "Single shot characterization of high transformer ratio wakefields in nonlinear plasma acceleration," *Phys. Rev. Lett.*, vol. 124, p. 044 802, 2020, doi:10.1103/PhysRevLett.124.044802

[10] C. A. Lindstrøm *et al.*, "Energy-spread preservation and high efficiency in a plasma-wakefield accelerator," *Phys. Rev. Lett.*, vol. 126, p. 014 801, 2021, doi:10.1103/PhysRevLett.126.014801

[11] C. Jing and G. Ha, "Roadmap for structure-based wakefield accelerator (swfa) r&d and its challenges in beam dynamics," *J. Instrum.*, vol. 17, T05007, 2022, doi:10.1088/1748-0221/17/05/T05007

[12] G. Ha, J. G. Power, J. Shao, M. Conde, and C. Jing, "Coherent synchrotron radiation free longitudinal bunch shaping using transverse deflecting cavities," *Phys. Rev. Accel. Beams*, vol. 23, p. 072 803, 2020, doi:10.1103/PhysRevAccelBeams.23.072803

[13] M. Cornacchia and P. Emma, "Transverse to longitudinal emittance exchange," *Phys. Rev. ST Accel. Beams*, vol. 5, p. 084 001, 2002, doi:10.1103/PhysRevSTAB.5.084001

[14] P. Emma, Z. Huang, K.-J. Kim, and P. Piot, "Transverse-to-longitudinal emittance exchange to improve performance of high-gain free-electron lasers," *Phys. Rev. ST Accel. Beams*, vol. 9, p. 100 702, 2006, doi:10.1103/PhysRevSTAB.9.100702

[15] G. Ha *et al.*, "Precision control of the electron longitudinal bunch shape using an emittance-exchange beam line," *Phys. Rev. Lett.*, vol. 118, p. 104 801, 2017, doi:10.1103/PhysRevLett.118.104801